Correspondence

Influence of Cell Line and Cell Cycle Phase on Sonoporation Transfection Efficiency in Cervical Carcinoma Cells Under the Same Physical Conditions

Samuel Pichardo, Melissa Togtema, Robert Jackson, Ingeborg Zehbe, and Laura Curiel

Abstract—Using cervical-carcinoma-derived cells as a model, the present study investigates the effects cell line and cell cycle phase have on sonoporation transfection efficiency under the same physical conditions. A plasmid expressing green fluorescent protein (GFP) was used to measure transfection efficiency. To evaluate the effect of cell type, CaSki, HeLa, and SiHa cells were sonoporated using an acoustic pressure of 1 MPa for 30 s with a duty cycle of 4.8% in the presence of the GFP plasmid. To study the effect of cell cycle phase, SiHa cells were synchronized at S-phase using a double thymidine block and sonoporated at different time points after the block. Contrast agent microbubbles were used at a 0.33% volume concentration. Results indicated that both cell line and cell cycle phase impact the transfection efficiency obtained with sonoporation.

I. Introduction

SONOPORATION is the process by which pores, or openings, are formed in the cell membrane under the effect of ultrasound exposure in the presence of micrometer-sized stabilized bubbles [1], such as the diagnostic contrast agent Definity (Lantheus Medical Imaging, North Billerica, MA). This process is transient, self-healing, and increases the permeability of the cell membrane, which allows the intracellular entry of various molecules including nucleic acids, proteins, and drugs [2]. Sonoporation has the potential to deliver gene therapeutic agents and there have been several studies employing this mechanism to deliver plasmid-DNA (pDNA), though reports on transfection efficiency differ from one study to another [3]–[6].

In this study, we analyzed the effects of cell line and cell cycle phase on sonoporation transfection efficiency under the same physical ultrasound parameters. Human papillomavirus (HPV)-positive cervical carcinoma cell lines were used as an *in vitro* model and sonoporation was employed to deliver green fluorescent protein (GFP) pDNA. There is little data regarding sonoporation of different cell lines using the same physical ultrasound parameters, because most studies have performed experiments with a single cell line only [6]. The choice of HPV-positive cervical carcinoma cell lines as a model is of great medical interest because virtually all cervical cancers contain high-risk HPV and persistent infection of the cervix with the virus is a necessary precursor to cervical cancer [7]. Sonoporation represents a considerable opportunity for a targeted, non-invasive delivery of macromolecules, such as antibodies, against oncoproteins coded for by the virus.

II. Materials and Methods

A. Ultrasound System

A 1-MHz transducer with a focal length of 72.4 mm and f-number of 0.86 was used for the experiments (PA242, Precision Acoustics Ltd., Dorset, UK). The efficiency of the transducer was measured to 85% using an analytical scale (PI-225D, Denver Instrument, Bohemia, NY) and an absorber attached to the scale [8]. The transducer was mounted on a robotic arm (UMS2, Precision Acoustics Ltd.) and a stationary arm secured the Opticell chamber (Thermo Fisher Scientific Inc., Waltham, MA). The exposure was done inside a water tank filled with degassed water (oxygen level $\leq$ 1 ppm) and temperature was maintained at 37°C using a closed-circuit heater. The distance between the transducer surface and the membrane to which the cells were adhered was 62.4 mm. This distance was chosen based on measurements of the acoustic pressure distribution done with a 0.2-mm-diameter needle hydrophone (SN1426, Precision Acoustics) to ensure a pressure distribution $\pm$10% with a central value of 1 MPa over a cross-sectional area of 6 mm diameter. The cross-section area at -6-dB was 8 mm in diameter. The exposure had a duration of 30 s with a duty cycle of 4.8% using a 30-cycle burst and a repetition rate of 1.6 kHz. These parameters were chosen based on previous studies [9] and a preliminary study was performed [10] to validate these parameters in SiHa cells. In that study, 6 pressure values were tested (0, 0.125, 0.25, 0.5, 0.75, and 1 MPa) with the same conditions of duty cycle as detailed previously and the pressure level of 1 MPa produced the largest level of transfection efficiency in the cells. To minimize standing wave effects, the absorber was placed 2 cm over the Opticell. The surface area of each Opticell chamber was divided into 24 randomly exposed regions with diameter of 6 mm each, which represents 27% of the total membrane surface area (50 cm²). Fig. 1 shows a diagram of the location of the exposures.
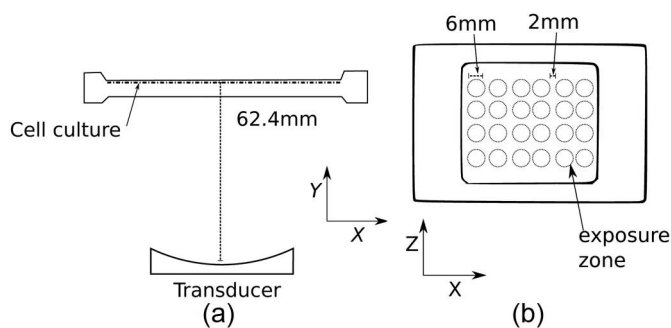
Fig. 1. Detail of the exposure setup. Twenty-four nonoverlapping exposure zones with a cross-sectional area of 8 mm in diameter at −6 dB were distributed over the surface area on the Opticell chamber.

B. Cell Lines, pDNA, and Microbubbles

SiHa, CaSki, and HeLa [American Type Culture Collection (ATCC), Manassas, VA], containing different HPV genotypes and number of viral copies [11]–[13], were maintained at 37°C, 5% CO_2 in 75-cm^2 flasks containing Dulbecco's modified Eagle's medium (DMEM; Sigma-Aldrich Canada Ltd., Oakville, ON, Canada) supplemented with 10% heat-inactivated fetal bovine serum (FBS; HyClone Laboratories Inc., Logan, UT) and 100 U of penicillin, 100 µg of streptomycin, and 0.25 µg amphotericin B per milliliter (antibiotic/antimycotic; Gibco, Grand Island, NY). Cells were passaged to sustain a 60% to 80% confluent monolayer. The 6.3-kb Omicslink pReceiverM03 plasmid containing the GFP gene (Genecopoeia Inc., Rockville, MD) was used to transform chemically competent NEB 5-α F'I^q *Escherichia coli* bacteria (New England BioLabs inc., Ipswich, MA). pDNA was extracted and purified using an EndoFree Plasmid Maxi Kit (Qiagen Inc., Toronto, ON, Canada).

For the delivery of the GFP plasmid DNA, cells were plated as a monolayer onto one side of an Opticell chamber with a concentration of 1.6×10^4 cells·cm^{-2}, 24 h before ultrasound exposure. The cells were then washed with serum- and antibiotic-free medium, and incubated with 250 µg of plasmid in 10 mL of serum- and antibiotic-free medium for 15 min at 37°C with 5% CO_2. Immediately preceding ultrasound exposure, 33 µL of activated Definity contrast agent was added to the Opticell and a waiting time of 1 min was observed [14]. After exposure, the Opticell was placed in the incubator for 2 h before the cells were returned to complete medium.

C. Gene Delivery Efficiency Per Cell Line

Twenty-four hours following ultrasound exposure, transfection efficiency for each cell line was determined as an average of the ratio of GFP-expressing cells to total cells. Groups of 2 Opticells for each cell type were organized as follows: ultrasound exposure in the presence of contrast agent, ultrasound exposure in the absence of contrast agent, and no ultrasound and the presence of contrast agent. Microscopy was performed using a Zeiss Ax-

iovert 200 inverted microscope and a 10× objective (Carl Zeiss Canada Ltd., North York, ON, Canada). Among 24 exposed regions per Opticell, efficiency was analyzed on 10 random fields of view. Two images were taken of each field of view—one phase contrast and one of the corresponding green fluorescence—using a 12-bit CCD camera (Q Imaging, Surrey, BC, Canada). Images were digitally processed using Northern Eclipse software version 8.0 (Empix Imaging Inc., Mississauga, ON, Canada).

D. Cell Viability Per Cell Line

Cell viability was calculated by comparing the number of adhered cells before and after procedure, and by evaluating the viability of remaining cells using the trypan blue dye exclusion test 24 h after procedure. Groups of 2 Opticells for each cell type were analyzed. Among 24 exposed regions, cells were counted on 10 random fields of view per Opticell both 15 min before and 2 h after sonoporation using phase-contrast microscopy. The total number of field of views was 20. The locations of the fields of view were in the treated region and were kept constant between time points. For the trypan blue dye exclusion, the cells were trypsinized 24 h after procedure. The cells were removed from the Opticell and resuspended in phosphate buffered saline (PBS). The cell suspension was mixed 1:1 with 0.4% trypan blue and the numbers of stained and unstained cells were counted using a TC10 automated cell counter (Bio-Rad, Mississauga, ON, Canada).

E. Cell Synchronization

SiHa cells were synchronized at the beginning of the synthesis (S) phase using a double thymidine block and were then treated with sonoporation at various time points following release from the block. Cells were seeded and grown for 24 h, after which thymidine was added to a final concentration of 2.5 mM and cells were incubated for 24 h (first block). Cells were released for 12 h in complete medium and then blocked a second time in 2.5 mM thymidine for another 24 h. The final release of the cells took place in complete medium for different lengths of time (0, 4, and 10.5 h). Flow cytometric analysis with propidium iodide staining using a FACScalibur flow cytometer (Becton, Dickinson and Co., Franklin Lakes, NJ) showed that the majority of cells at 0 h-release were in gap 1 (G1) and S phases, at 4 h-release were in S phase, and at 10.5 h-release were in the gap 2 and mitosis (G2&M) phase. Groups of 2 Opticells were synchronized at each of the indicated phases of the cell cycle. Nonblocked Opticells were used as a control. Images from 10 fields of view were collected for analysis from each synchronization time point.

F. Statistical Analysis

Statistical analysis was performed using *R*. Data were determined to meet parametric assumptions on the basis of normality and homogeneity of variance. Paramet-

ric data was analyzed using one-way analysis of variance (ANOVA) followed by Tukey's honestly significant difference (HSD) *post hoc* tests if significant global mean differences were found. Similarly, nonparametric data were analyzed using Kruskal–Wallis rank sum test followed by pairwise Wilcoxon rank sum tests. Significance level (α) was set, *a priori*, at 0.05.

III. Results

A. Influence of Cell Line

No cells exhibiting green fluorescence were observed in the control groups treated without contrast agent or in the absence of ultrasound. HeLa, SiHa, and CaSki cells showed average values ($\pm$ s.d.) of transfection efficiency of $7(\pm0.6)\%$, $6(\pm2)\%$, and $2.5(\pm0.2)\%$, respectively. *Post hoc* analysis demonstrated that CaSki cells had a significantly lower percentage of transfected cells than the other two cell lines ($p < 0.01$, $n = 10$). Mean values of percentage of remaining adhered cells were $-47 \pm 32\%$, $-38 \pm 42\%$, and $-75 \pm 32\%$ for SiHa, CaSki, and HeLa, respectively. The difference between cell lines was not significant ($p > 0.06$). The tryplan blue exclusion test was done 24 h following sonoporation to determine the viability of the cells which remained adhered. Ten counts were taken for each Opticell and then averaged. The remaining cells showed a viability of $93.4 \pm 4.1\%$, $92.6 \pm 3\%$, and $91 \pm 6\%$ for SiHa, CaSKi, and HeLa, respectively, and the results for each cell line were not significantly different from each other ($p > 0.60$).

B. Cell Cycle Phase Influence

The highest transfection efficiency was found when the majority of SiHa cells were at G2&M phase after blocking, with $14.4(\pm5.5)\%$ of cells transfected. The transfection efficiencies of nonblocked cells and cells synchronized in majority at G1/S and S phases demonstrated $6.9(\pm2)\%$, $6.5(\pm2.7)\%$, and $8.3(\pm2)\%$ transfection efficiencies, respectively. The transfection efficiency for cells synchronized at the G2&M phase was significantly higher compared with nonblocked cells ($p < 0.001$). Transfection efficiency for cells synchronized at the G1/S or S phases was not significantly different from the nonblocked cells ($p > 0.3$).

IV. Discussion and Conclusions

The present study indicates that the type of cervical cancer cell line has an impact on the transfection efficiency that can be achieved by sonoporation. This is in agreement with previous reports on other types of transfection techniques [15]. CaSki cells were the least susceptible to transfection with sonoporation. This observation suggests that the conditions required to induce the permeabilization of CaSki cell membranes using sonoporation must

be modified to recreate the same level of transfection observed for SiHa or HeLa cells. These results may have implications for a better design of therapeutic applications based on sonoporation. It is worth mentioning that the transfection efficiency was calculated on the population of cells that remained adhered after the procedure, which is consistent with previous reports [9], [16]. The difference of viability between cell lines was not significant and the observed values were in agreement with reported data [9], which indicated that the pressure level played a critical role in the viability. In that study (and under physical similar conditions to this report), the percentage of change of CHO cells was around -5% for 0.15 MPa and -20% for 0.5 MPa. The global average of the cell losses of SiHa, CaSki, and HeLa cells was -52%, which is about twice as much as the losses observed with CHO cells at 0.5 MPa. The choice of a considerably higher pressure helped to establish important evidence that the viability of cells is not dependent on the cell line. The trypan blue dye exclusion confirmed that the remaining attached cells, regardless of the cell line, remained with 90% or more viability.

The transfection efficiencies and cell viability found in our study are in agreement with previous studies where conditions to eliminate standing waves were also applied [4], [9]. In [9], Chinese hamster ovary (CHO) cells were also cultured using a monolayer setup and the observed transfection efficiency was 3%, using a peak-pressure of 250 kPa, duty cycle of 6%, and operating frequency of 1 MHz. In [4], C166 cells were sonoporated using an estimated peak-pressure of 125 kPa (authors reported an acoustic intensity at transducer surface of 4 W/cm^2, the pressure of 125 kPa was estimated assuming ideal conditions of sound propagation) with 100% duty cycle and the observed transfection efficiency was 5%. However, because the experimental setup is not exactly the same, a full extrapolation of these previous results to other cell lines is challenging. For purposes of studying new therapeutic modalities for HPV-related cervical cancer, it was important to study how the different cervical carcinoma cell lines responded to the exact same ultrasound parameters.

Cell cycle phase also had a considerable effect on the level of transfection efficiency obtained with sonoporation. When the majority of SiHa cells were at the G2&M phase, they were more susceptible to transfection. There is evidence that cell membrane potential is reduced during the M phase [17], which, in combination with sonoporation, may have produced increased membrane permeabilization. In a study using electroporation [18], authors reported that CHO cells at the G2&M phase were more susceptible to transfection. A previous conference proceeding [19] also reported the influence of the cell cycle phase on sonoporation transfection efficiency in unsynchronized fibrosarcoma KHT-C cells. Although their physical ultrasound parameters differed from ours, results obtained with our stringent standardization are in agreement with the notion that cells are most permeable to sonoporation during the G2&M phase.

References

[1] D. L. Miller and J. Quddus, "Sonoporation of monolayer cells by diagnostic ultrasound activation of contrast-agent gas bodies," *Ultrasound Med. Biol.*, vol. 26, no. 4, pp. 661–667, 2000.

[2] M. Kinoshita and K. Hynynen, "A novel method for the intracellular delivery of siRNA using microbubble-enhanced focused ultrasound," *Biochem. Biophys. Res. Commun.*, vol. 335, no. 2, pp. 393–399, 2005.

[3] T. Li, K. Tachibana, M. Kuroki, and M. Kuroki, "Gene transfer with echo-enhanced contrast agents: Comparison between Albunex, Optison, and Levovist in mice—Initial results," *Radiology*, vol. 229, no. 2, pp. 423–428, 2003.

[4] M. Kinoshita and K. Hynynen, "Key factors that affect sonoporation efficiency in in vitro settings: The importance of standing wave in sonoporation," *Biochem. Biophys. Res. Commun.*, vol. 359, no. 4, pp. 860–865, 2007.

[5] Y. S. Li, E. Davidson, C. N. Reid, and A. P. McHale, "Optimising ultrasound-mediated gene transfer (sonoporation) in vitro and prolonged expression of a transgene in vivo: Potential applications for gene therapy of cancer," *Cancer Lett.*, vol. 273, no. 1, pp. 62–69, 2009.

[6] J.M. Escoffre, A. Novell, A. Zeghimi, and A. Bouakaz "Ultrasound & microbubbles for in vitro gene delivery," *Drug Del. Tech.*, vol. 11, no. 3, pp. 42–47, 2011.

[7] H. zur Hausen, "Papillomaviruses and cancer: From basic studies to clinical application," *Nat. Rev. Cancer*, vol. 2, no. 5, pp. 342–350, 2002.

[8] K. Hynynen, "Acoustic power calibrations of cylindrical intracavitary ultrasound hyperthermia applicators," *Med. Phys.*, vol. 20, no. 1, pp. 129–134, 1993.

[9] A. Rahim, S. L. Taylor, N. L. Bush, G. R. ter Haar, J. C. Bamber, and C. D. Porter, "Physical parameters affecting ultrasound/microbubble-mediated gene delivery efficiency in vitro," *Ultrasound Med. Biol.*, vol. 32, no. 8, pp. 1269–1279, 2006.

[10] L. Curiel, K. Lee, S. Pichardo, and I. Zehbe, "Sonoporation of cervical carcinoma cells affected with E6-oncoprotein for the treatment of uterine cancer," *AIP Conf. Proc.*, vol. 1215, pp. 119–122, 2010.

[11] F. Friedl, I. Kimura, T. Osato, and Y. Ito, "Studies on a new human cell line (SiHa) derived from carcinoma of uterus. I. Its establishment and morphology," *Proc. Soc. Exp. Biol. Med.*, vol. 135, no. 2, pp. 543–545, 1970.

[12] R. A. Pattillo, R. O. Hussa, M. T. Story, A. C. Ruckert, M. R. Shalaby, and R. F. Mattingly, "Tumor antigen and human chorionic gonadotropin in CaSki cells: A new epidermoid cervical cancer cell line," *Science*, vol. 196, no. 4297, pp. 1456–1458, 1977.

[13] N. C. Popescu, J. A. DiPaolo, and S. C. Amsbaugh, "Integration sites of human papillomavirus 18 DNA sequences on HeLa cell chromosomes," *Cytogenet. Cell Genet.*, vol. 44, no. 1, pp. 58–62, 1987.

[14] D. L. Miller, C. Dou, and J. Song, "DNA transfer and cell killing in epidermoid cells by diagnostic ultrasound activation of contrast agent gas bodies in vitro," *Ultrasound Med. Biol.*, vol. 29, no. 4, pp. 601–607, 2003.

[15] K. L. Douglas, C. A. Piccirillo, and M. Tabrizian, "Cell line-dependent internalization pathways and intracellular trafficking determine transfection efficiency of nanoparticle vectors," *Eur. J. Pharm. Biopharm.*, vol. 68, no. 3, pp. 676–687, 2008.

[16] I. Lentacker, B. Geers, J. Demeester, S. C. De Smedt, and N. N. Sanders, "Design and evaluation of doxorubicin-containing microbubbles for ultrasound-triggered doxorubicin delivery: Cytotoxicity and mechanisms involved," *Mol. Ther.*, vol. 18, no. 1, pp. 101–108, 2009.

[17] H. G. Sachs, P. J. Stambrook, and J. D. Ebert, "Changes in membrane potential during the cell cycle," *Exp. Cell Res.*, vol. 83, no. 2, pp. 362–366, 1974.

[18] M. Golzio, J. Teissié, and M. P. Rols, "Cell synchronization effect on mammalian cell permeabilization and gene delivery by electric field," *BBA-Biomembranes*, vol. 1563, no. 1–2, pp. 23–28, 2002.

[19] R. Karshafian, P. Bevan, G. Czarnota, and P. Burns, "The dependence of sonoporation on cell cycle phase: Enhanced effect during G2 and S-phase," in *IEEE Ultrasonics Symp.*, 2007, pp. 2005–2008.